Myosin-1a powers the sliding of apical membrane along microvillar actin bundles

Russell E. McConnell and Matthew J. Tyska

Department of Cell and Developmental Biology, Vanderbilt University Medical Center, Nashville, TN 37232

Microvilli are actin-rich membrane protrusions common to a variety of epithelial cell types. Within microvilli of the enterocyte brush border (BB), myosin-1a (Myo1a) forms an ordered ensemble of bridges that link the plasma membrane to the underlying polarized actin bundle. Despite decades of investigation, the function of this unique actomyosin array has remained unclear. Here, we show that addition of ATP to isolated BBs induces a plus end–directed translation of apical membrane along microvillar actin bundles. Upon reaching microvillar tips, membrane is "shed" into solution in the form of small vesicles. Because this movement demonstrates the polarity, velocity, and nucleotide dependence expected for a Myo1a-driven process, and BBs lacking Myo1a fail to undergo membrane translation, we conclude that Myo1a powers this novel form of motility. Thus, in addition to providing a means for amplifying apical surface area, we propose that microvilli function as actomyosin contractile arrays that power the release of BB membrane vesicles into the intestinal lumen.

Introduction

Microvilli are actin-rich membrane protrusions common to all transporting and sensory epithelial cell types. The brush border (BB) domain found at the apex of the enterocyte consists of thousands of tightly packed microvilli that extend off of the apical surface to a uniform length. In the BB, each microvillus is supported by a polarized bundle of actin filaments that are linked to the overlying apical membrane by an ensemble of the membrane-binding motor protein, myosin-1a (Myo1a, originally brush border myosin I; Mooseker and Tilney, 1975; Mooseker and Coleman, 1989). While the cellular role of this array remains unclear, BBs in mice lacking Myo1a demonstrate a variety of defects; among the most striking are herniations of apical membrane, irregularities in microvillar packing, and abnormal variability in microvillar length (Tyska et al., 2005). The mechanistic details underlying these phenotypes and specifically, the involvement of Myo1a motor activity, has yet to be elucidated.

Microvilli share structural features with other actin-rich membrane protrusions such as filopodia and stereocilia. In all of these cases, parallel bundles of actin filaments provide the structural core and mechanical support for the membrane extension (Revenu et al., 2004). The uniform polarity of filaments in these structures suggests that supporting bundles could serve as tracks for the polarized movement of motor proteins. Indeed, recent studies have demonstrated that myosin-X undergoes motor-driven movements toward the tips of filopodia (Berg and Cheney, 2002). In a similar manner, the motor activity of myosin-XVa is thought to drive its accumulation at the tips of stereocilia (Belyantseva et al., 2003; Rzadzinska et al., 2004). Moreover, recent data from Yang et al. (2005) demonstrate that, in the context of the kidney proximal tubule, acute hypertension induces a redistribution in myosin-VI (Myo6) immunoreactivity from microvillar tip to base, implying that this motor may use the core bundle as a track for minus end–directed movement.

While Myo1a demonstrates mechanical activity in the sliding filament assay (Wolenski et al., 1993b), there is currently no data on the ability of Myo1a to move apical membrane or translate membrane components along microvillar actin bundles. Based on the geometry of the microvillus (Mooseker and Tilney, 1975) and the known mechanical properties of Myo1a (Wolenski et al., 1993a), we predict that the ensemble of Myo1a in the microvillus represents a contractile array, exerting plus end–directed force on the apical membrane. In vivo, these forces could be engaged for the intramicrovillar trafficking of membrane lipids and proteins, or perhaps other unexplored roles.

We sought to test our prediction by investigating isolated BBs under conditions expected to stimulate the mechanical activity of Myo1a. Data from time-lapse imaging studies, ultrastructural analysis, and biochemical assays all indicate that the
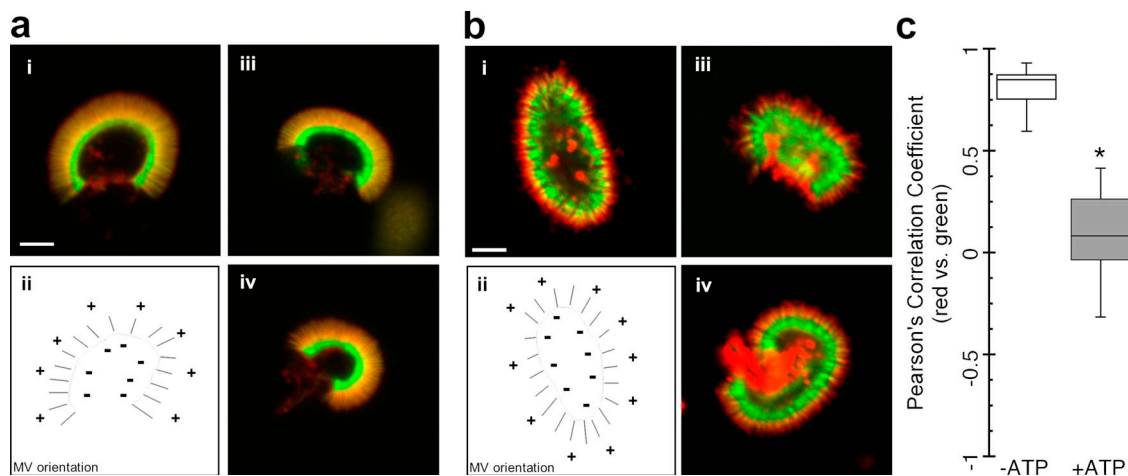
Figure 1. **ATP induces apical membrane redistribution in isolated BBs.** (A) Laser scanning confocal sections of isolated BBs (i, iii, and iv) demonstrate the normal overlap of membrane (TRITC-ConA, red) and actin (Alexa488-phalloidin, green). (B) BBs treated with 2 mM ATP and then fixed 5 min later show an accumulation of membrane at microvillar tips (i.e., core bundle plus-ends). In both A and B, cartoons in panel ii show the arrangement of microvillar (MV) actin bundles for the BB in panel i. (C) Pearson correlation coefficients were calculated for the red (membrane) and green (actin) fluorescence images from untreated and ATP-treated BBs. Correlation coefficients are plotted as box plots; solid line within the box corresponds to the median, edges of the box are the 25th and 75th percentiles, and whiskers are the 10th and 90th percentiles. Mean coefficients were 0.81 ± 0.10 (mean ± SD, n = 14) for un-treated BBs and 0.08 ± 0.21 (n = 13) for ATP-treated BBs. ATP treatment significantly reduced (*, P < 0.00001) the correlation between these two signals. Bars (A and B), 2.5 μm.

microvillar array of Myo1a is mechanically active and exerts substantial plus end–directed force on the apical membrane. In isolated BBs, this force is manifest as a rapid plus end–directed sliding of apical membrane along microvillar actin bundles. The translation of apical membrane ultimately results in the release of vesicles from microvillar tips. These studies demonstrate that microvillar actin bundles are a suitable substrate for myosin-based movement and that Myo1a produces mechanical force sufficient to power the movement of apical membrane over the

actin cytoskeleton. Intriguingly, these data may also provide a mechanism for the appearance of BB membrane vesicles in the lumen of the small intestine (Jacobs, 1983). Thus, in addition to providing a means for amplifying apical surface area, we propose that microvilli function as actomyosin contractile arrays, powering the release of BB membrane vesicles into the intestinal lumen. This activity may have implications with regard to the general efficiency of nutrient processing and other critical aspects of gastrointestinal physiology.
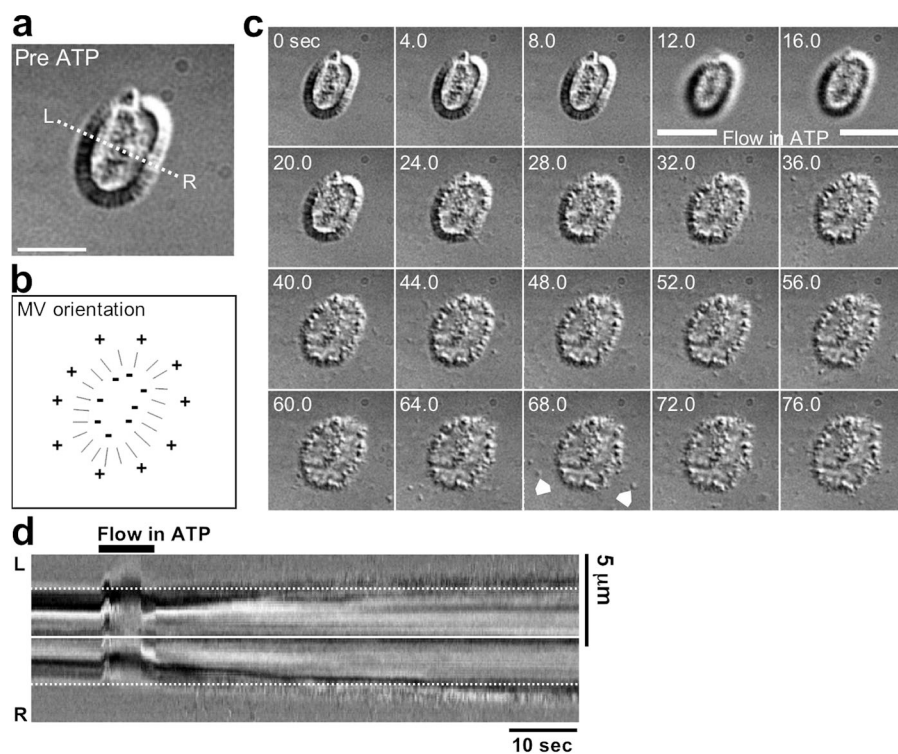

Figure 2. **Time-lapse analysis of ATP-induced BB membrane redistribution.** (A) DIC micrograph of an isolated BB mounted in a flow cell before ATP treatment. Bar, 5 μm. (B) Schematic of the BB in A showing the orientation of microvillar (MV) actin bundles. (C) Time-lapse DIC image series of the same BB in panel A before (t = 0–8 s), during (t = 12–16 s), and after (t = 20–76 s) the addition of 2 mM ATP. Addition of ATP stimulates the translation of membrane toward microvillar tips located at the BB periphery. Membrane vesicles are also seen accumulating in solution surrounding the BB (white arrowheads at 68s). (D) Kymograph generated from a line drawn parallel to the microvillar axis (A, dashed line) shows movement of the BB membrane (y-axis) over time (x-axis); membrane translates away from the BB center (solid line) toward the actin plus-ends at the MV tips (dotted lines).

Results

ATP induces the redistribution of apical membrane in isolated BBs

To determine if microvillar Myo1a is mechanically active, we first examined the impact of ATP on the structure of BBs isolated from rat small intestine. For these studies, phalloidin-stabilized BBs were exposed to saturating (2 mM) levels of ATP in the presence of 1 mM EGTA; this chelator was included because Ca^{2+} is known to depress the mechanical activity of Myo1a in vitro, via effects on bound calmodulin light chains (Wolenski et al., 1993b). BBs were fixed 5 min after ATP addition, labeled with ConA, and examined using laser scanning confocal microscopy. These observations revealed that ATP treatment induced a striking accumulation of apical membrane at microvillar tips (i.e., actin bundle plus-ends; Fig. 1). This was confirmed quantitatively as a significant loss in the correlation coefficient calculated from the BB membrane and actin probe fluorescence signals (Fig. 1 C). In many BBs, we also observed terminal web contraction, an established form of myosin-II (Myo2) mechanical activity (Rodewald et al., 1976; Burgess, 1982; Keller and Mooseker, 1982).

ATP-induced membrane redistribution is the result of plus end–directed translation

To examine the dynamics of apical membrane redistribution induced by ATP, we used time-lapse differential interference contrast (DIC) microscopy. BBs were immobilized within a flowcell and imaged with the long axis of microvilli parallel to the focal plane (Fig. 2, A and B). When 2 mM ATP was perfused through the flowcell we observed a robust, centrifugal expansion of the refractile bands that represent apical membrane (Fig. 2 C; Video 1, available at http://www.jcb.org/cgi/content/full/jcb.200701144/DC1). Kymographs formed from a line that bisects the BB (Fig. 2 D) clearly show that the bands of apical membrane translate away from the center of the structure. Movement began immediately after ATP addition and continued rapidly in the first minute of observation. After ~1 min, movement slowed as membrane reached a distance equivalent to the original position of microvillar tips (Fig. 2 D, white dashed lines). Although these observations suggest that ATP stimulates the translation of apical membrane along microvillar actin bundles, we sought to confirm this by performing time-lapse fluorescence microscopy of BBs labeled with probes specific to the apical membrane and actin cytoskeleton. Indeed, spinning disk confocal microscopy (SDCM) of double-labeled BBs confirmed that ATP stimulates a robust translation of apical membrane toward microvillar tips (Fig. 3, A and B; Video 2). Kymographs of the resulting time series demonstrated that the length of microvillar actin bundles is unaffected during this process (Fig. 3 B). Moreover, when the velocity of membrane movement was tallied from multiple kymographs, we obtained a mean membrane translation velocity of 19.2 ± 6.1 nm/s (Fig. 3 C). These data indicate that ATP induces movement of apical membrane with a polarity and velocity that are consistent with the activity of a class I myosin (Coluccio, 1997).

ATP-induced membrane translation gives rise to vesiculation at microvillar tips

Kymograph analysis of SDCM time-lapse data shows that the band representing apical membrane narrows as it translates toward microvillar tips, indicating an overall loss of BB-associated membrane after ATP addition (Fig. 3 B). One explanation for this loss is that membrane is pushed off of microvillar tips, resulting in its vesiculation or "shedding" from the BB. Indeed, the DIC images presented above (Fig. 2) reveal that ATP-stimulated membrane movement is accompanied by an extensive release of material resembling small vesicles (Fig. 2 C, arrowheads at 68 s). Consistent with these data, SDCM images that are contrast adjusted to enable visualization of dim material reveal a cloud of vesicles in solution around the BB after ATP addition (Fig. 3 D). When total solution fluorescence is monitored throughout the time lapse, a burst in signal intensity is observed coinciding with the addition of ATP (Fig. 3 E). These data
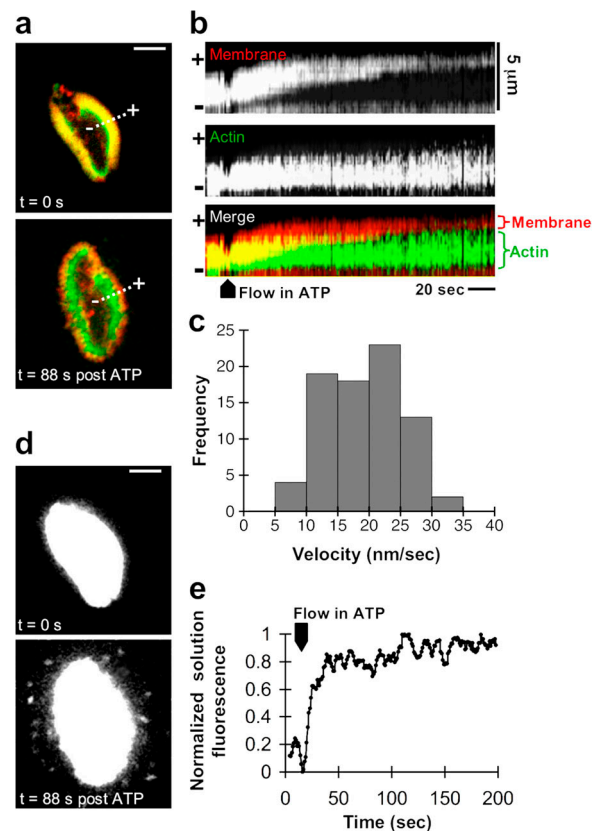

Figure 3. **ATP stimulates the plus end–directed translation of membrane over microvillar actin bundles.** (A) Spinning disk confocal micrographs of a fluorescently labeled BB (Alexa488-ConA, membrane, red; Alexa546-Phalloidin, actin, green) before (t = 0 s) and after (t = 88s) addition of 2 mM ATP; the accumulation of membrane at microvillar tips can clearly be observed after ATP addition. (B) Kymographs drawn from the white dashed line over the BB in panel A reveal that membrane (red) moves toward the microvillar tips as the actin bundle length (green) remains constant. (C) Histogram of membrane translation velocities derived from 79 kymographs of 42 BBs; mean velocity equals 19.2 ± 6.1 nm/s (mean ± SD). (D) Contrast enhancement of the membrane (red) channel in panel A reveals an accumulation of small membrane vesicles in solution around the BB after ATP treatment. (E) Quantification of integrated fluorescence in solution surrounding the BB shows a release of membrane that begins immediately after the addition of 2 mM ATP. Bars (A and D), 5 μm.
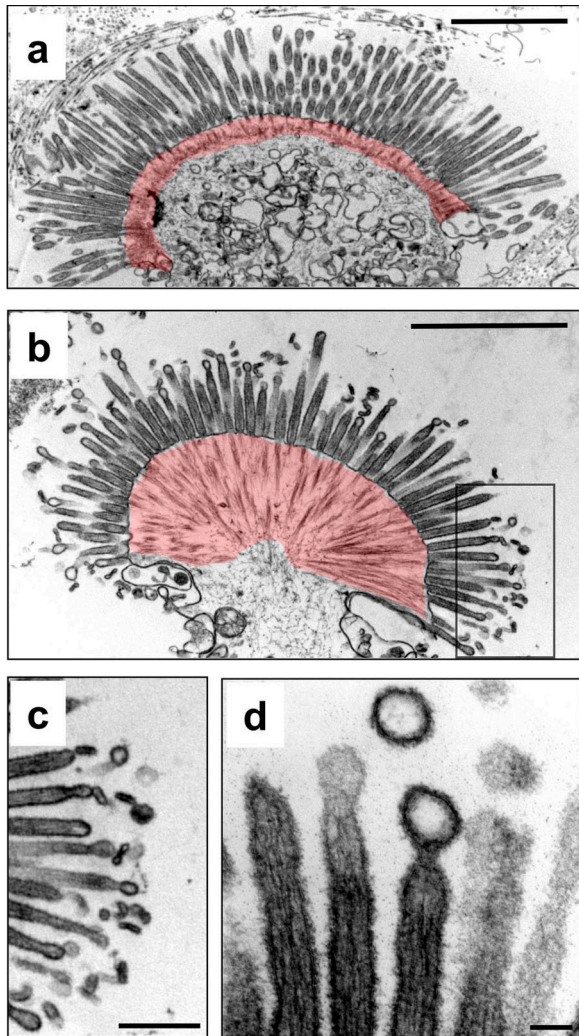
Figure 4. **Ultrastructural analysis of BB membrane shedding.** (A) TEM analysis of an isolated BB shows that the apical membrane covers the majority of the core actin bundles, leaving only a small fraction of their length exposed at bundle minus-ends (region highlighted in red). (B) BB from the same preparation as in panel A after treatment with 2 mM ATP. In addition to extensive vesiculation at microvillar tips, a significantly greater length of individual actin bundles appear to be exposed (i.e., membrane free) at the bundle minus-ends (compare red regions in A and B). (C) Higher magnification view of boxed area in panel B clearly shows vesiculation at the tips of nearly all microvilli. (D) Vesicles shed from tips exhibit a diameter comparable to the microvillus and show no evidence of actin bundle fragments at their core. Bars: (A and B) 2 μm; (C) 0.5 μm; (D) 0.1 μm.

indicate that membrane shedding occurs in parallel with membrane translation.

We expect membrane shedding to take place at microvillar tips, as membrane accumulates in this region after ATP addition (Figs. 1–3). To further characterize the BB response to ATP and unambiguously determine the location of membrane release, we performed ultrastructural analysis on ATP-treated BBs. Transmission electron microscopy (TEM) revealed extensive vesiculation of the apical membrane at microvillar tips in the presence of ATP (Fig. 4, A and B). Vesiculation was widespread and observed at the tip of nearly every microvillus (Fig. 4 C). High magnification panels revealed that vesiculating membrane was devoid of electron-dense material and exhibited

a diameter comparable to that of the microvillus (∼100 nm; Fig. 4 D). ATP treatment also resulted in the exposure of a greater length of actin bundle at the base of microvilli. In the absence of ATP, microvillar actin bundles typically extend into the terminal web by only a small fraction of their total length (10–20% of total length; Fig. 4 A, red region). After ATP activation, microvillar bundles in most BBs were observed with ≥50% of their total length exposed and extending into the terminal web (Fig. 4 B, red region). In other cases, we observed actin bundles that were completely stripped of membrane, yet positioned adjacent to an accumulation of vesicles (unpublished data). These ultrastructural analyses show that ATP-induced membrane translation gives rise to membrane shedding from microvillar tips.

Characterization of vesicles released during ATP-induced membrane shedding

Our ultrastructural observations suggest that the vesicles released from microvillar tips after ATP treatment represent parcels of apical membrane. To further characterize the composition and properties of shed vesicles, we used differential centrifugation to fractionate ATP-treated BBs. When BBs were incubated in the presence or absence of ATP and then sedimented at 5,000 g, membrane markers (sucrase-isomaltase [SI] and alkaline phosphatase [AP]) and Myo1a were released into the supernatant only in the presence of ATP (Fig. 5 A). Moreover, all of the SI and AP in the 5,000-g supernatant sedimented at 100,000 g, suggesting that these components are indeed membrane associated (Fig. 5 A). A significant fraction (∼20%) of the Myo1a released with ATP addition also sedimented at 100,000 g, indicating that a subpopulation of this motor remains bound to the apical membrane during the time course of ATP-induced membrane translation and shedding (Fig. 5 A). The appearance of vesicles in ATP-treated preparations was also confirmed using TEM analysis; an abundance of vesiculated membrane material appeared in the 5,000-g supernatant only after BBs were treated with ATP (Fig. 5 B). In addition, examination of the 100,000-g pellet showed that this fraction is enriched in small vesicles ranging from 50–200 nm in diameter, comparable to those observed in ultrastructural analyses of ATP-treated BBs (Fig. 5 C).

A quantitative assay for BB membrane shedding

To further investigate the mechanism of BB membrane shedding, we devised a quantitative membrane shedding assay (MSA). This assay allowed us to quantify the release of apical membrane vesicles produced by a large population of BBs, under a variety of biochemical conditions and perturbations. BBs were labeled with the lipophilic fluorescent dye AM1-43 and then activated to shed with the addition of ATP. After 2 min, vesiculated membrane was separated from BB remnants with a centrifugation step and the resulting supernatant transferred to a 96-well microplate for the measurement of AM1-43 fluorescence (Fig. 6 A). Importantly, AM1-43 labeling appeared uniform within and between individual BBs (Fig. 6 B), and the ATP-dependent signal scaled linearly with the quantity of BB in the reaction (Fig. 6 C).
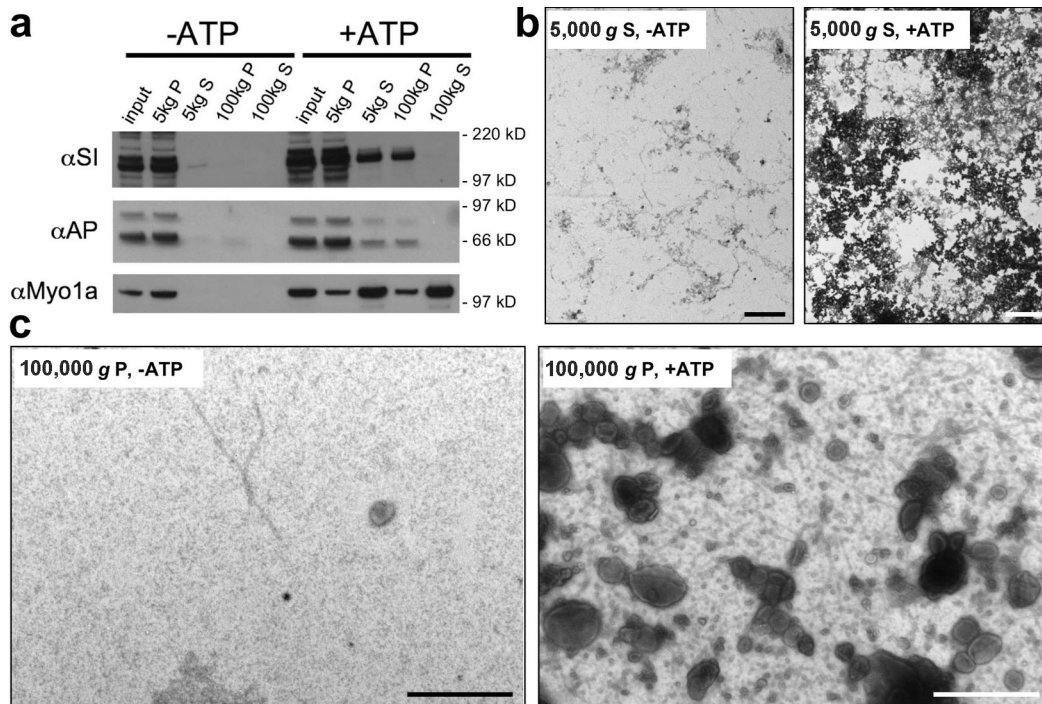
Figure 5. **Characterization of vesicles released from the BB upon ATP treatment.** (A) BB samples in the presence or absence of ATP were fractionated using differential centrifugation and then separated using SDS-PAGE. Western blots show that apical membrane markers, SI and AP, undergo ATP-induced redistribution from the low speed (5,000 g) pellet (P) into the low speed supernatant (S). Ultraspeed centrifugation (100,000 g) of the 5,000-g S fraction reveals that both membrane markers sediment, indicating membrane association. Although Myo1a is also released from the BB in the presence of ATP, a significant amount of Myo1a sediments with membrane markers in the 100,000-g P fraction. (B) TEM of the negatively stained 5,000-g S fraction shows that ATP induces the release of copious amounts of membrane material. (C) TEM of negatively stained 100,000-g P fraction confirms the presence of small vesicles similar in appearance to those observed in micrographs of isolated BBs. Bars: (B) 2 μm; (C) 0.5 μm.

BB membrane shedding exhibits the nucleotide dependence expected for a myosin-driven process

To determine if ATP-induced membrane translation and shedding are powered by an ATPase such as Myo1a, we used the MSA to examine the nucleotide dependence of this activity. In the absence of ATP, ADP and PPi were unable to activate membrane shedding (Fig. 7 A). Next, we determined if ATP hydrolysis was required to activate membrane shedding by carrying out the MSA with the nonhydrolyzable ATP analogues, ATPγS and AMP-PNP. These analogues produced only a fraction of the response observed for an equivalent concentration of ATP, indicating that hydrolysis is required to fully activate membrane shedding (Fig. 7 A). The remnant response observed in the case of both analogues (~10–20% of ATP control) could be due to the low concentration of contaminating ATP in these analogue preparations. Alternatively, it may indicate that ATP binding alone accounts for a small fraction of total membrane shedding.

Myosin mechanical activity is known to demonstrate Michaelis-Menten dependence with respect to ATP concentration (Howard, 2001). If BB membrane shedding is powered by a motor such as Myo1a, it should also demonstrate such dependence. To test this, we examined the rate of membrane shedding over a wide range of ATP concentrations. Indeed, these experiments revealed that shedding (Fig. 7 B) exhibits hyperbolic dependence with respect to ATP concentration. Fitting these data to a Michaelis-Menten model (normalized shedding = V_{Max}*[ATP]/K_M + [ATP]) yields a V_{Max} of 1.2 ± 0.1 mM and a K_M (for ATP) of 396 ± 103 μM. We also examined the impact of the hydrolysis product, ADP, on shedding activity in the presence of saturating levels of ATP. In vitro biochemical studies on other myosin motors have established that ADP serves as a pure competitive inhibitor of ATPase activity (Kelemen, 1979). Consistent with this prediction, the presence of 2 mM ADP increased the K_M with respect to ATP approximately fivefold, while V_{Max} was unaffected (Fig. 7 B, inset). This shift in K_M enabled us to calculate an ADP K_I of 554 μM (from $K_I = K_M$ [ADP]/$K_M' - K_M$). This value is slightly higher but comparable to that determined for smooth muscle Myo2 (in the sliding filament assay), a myosin that exhibits high affinity for ADP in a manner similar to Myo1a (Warshaw et al., 1991; Jontes et al., 1997; Cremo and Geeves, 1998).

ATP-induced membrane shedding is independent of Myo2 activity

The nucleotide dependence of membrane shedding suggests that this process is powered by a myosin ATPase. Thus, we wanted to determine if Myo2, the most abundant myosin in the BB, plays a role in driving this activity. For these experiments, we performed the MSA in the presence of 50 μM blebbistatin, an established Myo2 inhibitor (Straight et al., 2003; Kovacs et al., 2004). Consistent with the known localization of Myo2 in the terminal web, blebbistatin had no observable impact on the extent of membrane shedding from microvillar tips (Fig. 7 C).
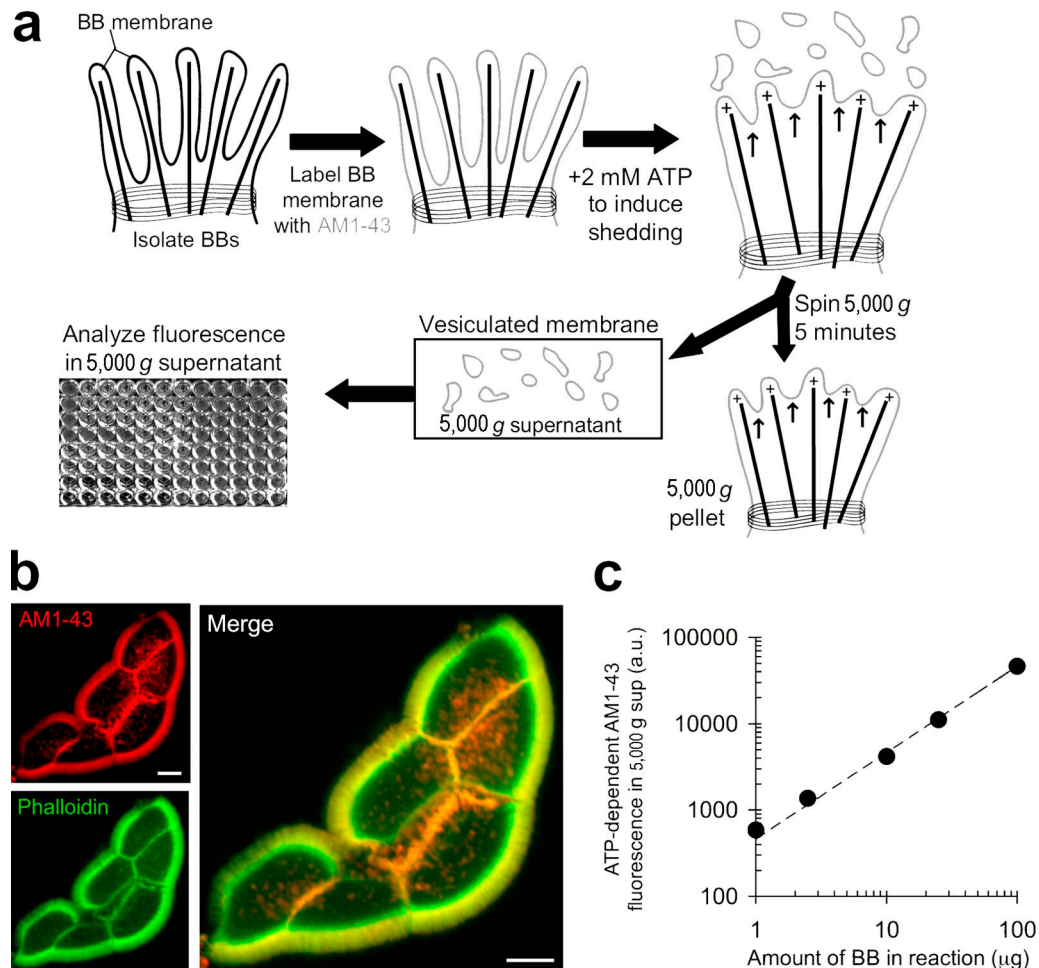
Figure 6. **Quantitative assay for BB membrane shedding.** (A) Schematic of the assay used to quantify the extent of BB membrane shedding under various conditions. BBs are labeled with AM1-43, reacted with 2 mM ATP, centrifuged to isolate the shed membrane (5,000-*g* supernatant), and the amount fluorescent material is measured in a microplate reader. (B) Laser scanning confocal micrograph of phalloidin-labeled (green) isolated BBs shows that AM1-43 (red) evenly labels the BB membrane. Bars, 4 μm. (C) Increasing concentrations of BBs were treated with 2 mM ATP and the amount of membrane shed from each sample was measured using the microplate assay. ATP-induced membrane shedding scales with the BB concentration, demonstrating a linear response over two orders of magnitude. Points on this plot represent mean ± SD calculated from replicates at each BB concentration (for all values, SD is smaller than the point size).

Moreover, in the presence of blebbistatin, BBs lacked the tight curvature normally produced by ATP addition (compare Fig. 7 D with Fig. 4 B), indicating that terminal web contraction (Rodewald et al., 1976; Burgess, 1982; Keller and Mooseker, 1982; Keller et al., 1985), and thus Myo2 activity, were indeed inhibited. These data indicate that ATP-induced membrane translation and shedding are Myo2-independent activities.

ATP-induced membrane shedding is Myo1a dependent

Given its established membrane binding potential (Hayden et al., 1990; Zot, 1995), high density in the microvillus (Bretscher, 1991), and polarity of movement (Wolenski et al., 1993a), Myo1a is the most obvious candidate for powering the plus end–directed movement and shedding of membrane induced by ATP. Indeed, our previous studies have shown that BBs from Myo1a knock-out (KO) mice are not "damaged" to the same extent as wild-type (WT) BBs when exposed to ATP (Tyska et al., 2005). Thus, we investigated the involvement of Myo1a in the membrane shedding response by performing the MSA with

BBs isolated from the small intestine of Myo1a knock-out (KO) mice (Tyska et al., 2005) and age-matched wild-type (WT) controls (Fig. 7 E). Strikingly, the shedding response of Myo1a KO BBs was only a small fraction (~5%) of that exhibited by WT BBs (Fig. 7 F). The difference in activity was not due to disparity in AM1-43 labeling efficiency as labeled WT and KO BBs exhibited comparable levels of fluorescence (Fig. 7 G). Moreover, visual observation of the response to ATP confirmed that KO BBs failed to carry out the plus end–directed membrane translation and shedding normally observed in WT BBs (Fig. 7 H). Together these data strongly indicate that Myo1a is required for the ATP-stimulated membrane movement and vesiculation observed in isolated BBs.

Discussion

A novel contractile activity in the microvillus

In this paper, we describe a novel form of microvillar contractility that can be reactivated by exposing native, isolated BBs to ATP.
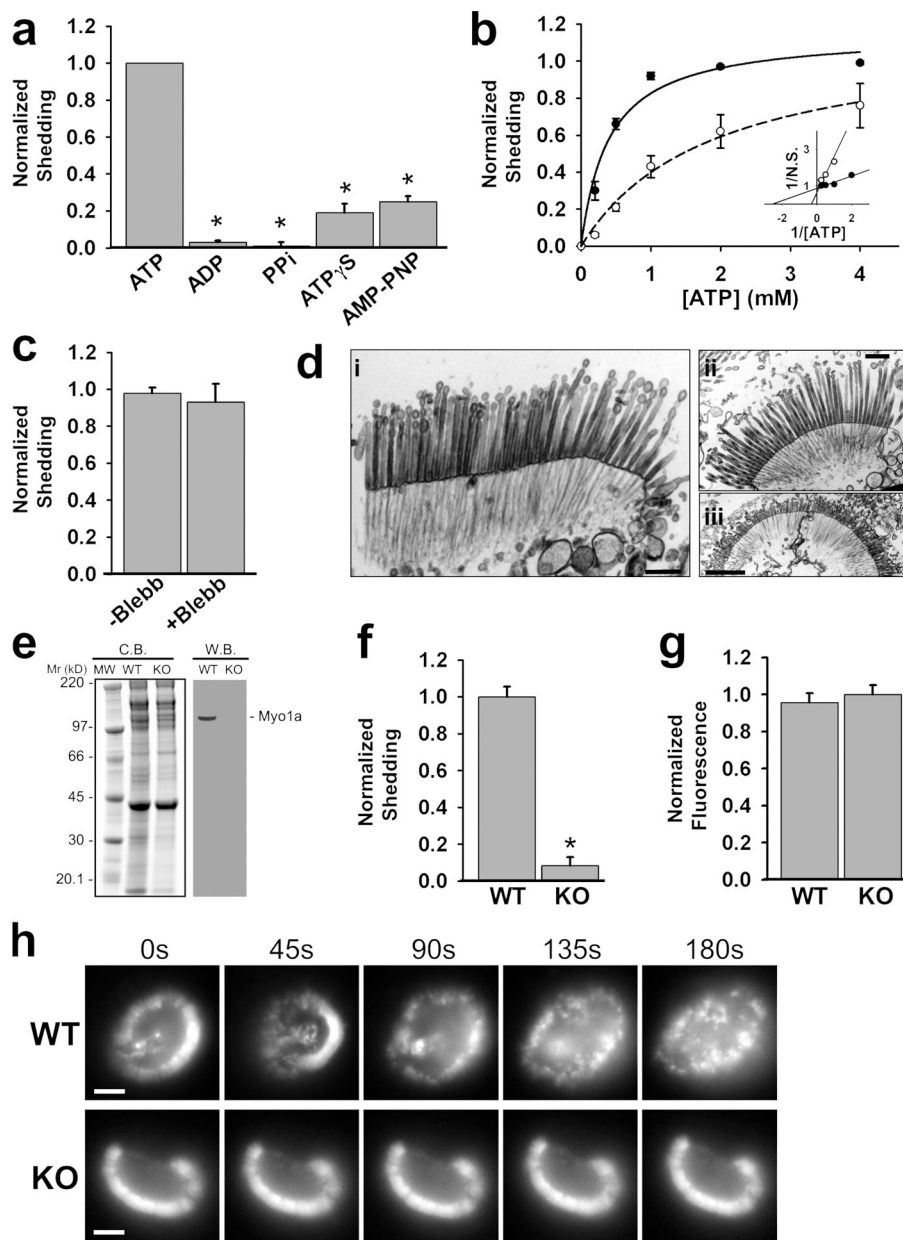
Figure 7. **Nucleotide and myosin dependence of BB membrane shedding.** (A) 20 μg/ml BBs were treated with 2 mM of ATP, adenosine diphosphate (ADP), pyrophosphate (PPi), adenosine 5′-[γ-thio] triphosphate (ATPγS), or adenosine 5′-[β,γ-imido] triphosphate (AMP-PNP), and membrane shedding was quantified using the MSA. ATP strongly stimulated membrane shedding, while ADP and PPi had essentially no effect, and the nonhydrolyzable ATP analogues ATPγS and AMP-PNP evoked only minor responses. (B) Membrane shedding exhibits Michaelis-Menten kinetics with respect to ATP concentration (closed circles, solid line shows curve fit; $V_{Max} = 1.2 \pm 0.1$ mM, $K_M = 396 \pm 103$ μM). In the presence of 2 mM ADP (open circles, dashed line shows curve fit; $V_{Max} = 1.1 \pm 0.1$ mM, $K_M = 1,869 \pm 437$ μM), membrane shedding is inhibited. Inset shows the double-reciprocal plot of the same data. (C) Incubating BBs with 50 μM Blebbistatin, a potent Myo2 inhibitor, has no effect on membrane shedding as measured in the MSA. (D) TEM analysis of BBs incubated with 50 μM Blebbistatin and 2 mM ATP (i–iii) shows that the junctional contraction associated with Myo2 activity is absent, as indicated by the parallel orientation of microvillar actin bundles in these BBs (compare with Fig. 4 B). However, the robust vesiculation at microvillar tips appears unaffected by Blebbistatin. (E) Coomassie blue (C.B.)–stained gel of WT and Myo1a KO BB fractions and associated anti-Myo1a Western blot (W.B.) confirms the absence of Myo1a in KO samples. (F) ATP-induced membrane shedding measured for equal quantities (5 μg) of WT and Myo1a KO BBs. KO BBs exhibit ~5% of the shedding activity seen in WT BBs. (G) The fluorescence signals measured from equal amounts (5 μg) of WT and Myo1a KO BBs show equivalent labeling by AM1-43. (H) BB membranes were fluorescently labeled with Alexa488-ConA, treated with 2 mM ATP, and imaged for 3 min. Time-lapse images show that the WT BB exhibits a robust loss of membrane, yet the KO BB membrane structure remains essentially unchanged during this time course. For the values plotted in A–C, each point represents the mean ± SD calculated from at least three different BB preparations. The values plotted in F and G represent mean ± SD calculated from replicates of the same BB preparation, but are representative of five individual paired WT and KO BB preparations. Bars: 0.5 μm (di, ii); 2 μm (diii, h). *, P < 0.05.

Reactivation is manifest as the plus end–directed movement of apical membrane along microvillar core actin bundles, and eventually, the accumulation of membrane at microvillar tips. Upon reaching the tips, the membrane no longer maintains contact with the underlying actin cytoskeleton and vesiculation is favored; small vesicles that contain Myo1a and are enriched in other apical membrane markers are released into solution (Fig. 8 A). The translation and shedding of membrane requires ATP hydrolysis, demonstrates the nucleotide dependence expected for a myosin ATPase, and is substantially depressed in the absence of Myo1a. Intriguingly, the membrane translation velocities (Fig. 3 B; 19.2 ± 6.1 nm/s) measured here are nearly identical to velocities measured in sliding filament assays with Myo1a immobilized on lipid-coated coverslips (Wolenski et al., 1993b).

Myo1a is a good candidate for driving this novel form of motility, as previous studies have established that this motor can bind directly to apical membrane lipids (Hayden et al., 1990; Zot, 1995) and proteins (Tyska and Mooseker, 2004), is present at a very high concentration (>70 μM) in the microvillus (Bretscher, 1991), and moves toward the plus-ends of actin filaments in vitro (Wolenski et al., 1993a). Thus, in combination with previous studies, our data strongly indicate that Myo1a is the motor that powers ATP-stimulated membrane translation and shedding in isolated BBs.

Our findings demonstrate that the polarized actin bundles that support microvilli serve as tracks for myosin-based motor activity. Although these studies focus on Myo1a, a reasonable extension of this is that other myosins in the BB

Figure 8. **BB membrane shedding model.** (A) In isolated BBs, Myo1a motor activity powers the translation of apical membrane toward the actin bundle plus-end at the microvillus tip. Upon reaching the tip, membrane vesiculates and is shed from the BB. (B) In the context of an intact enterocyte, Myo1a-powered membrane translation may underlie the regulated turnover of BB membrane. New membrane is continually delivered to the terminal web, while older membrane is translated along microvillar actin bundles and eventually released from tips, into the intestinal lumen.

t = 0   t > 0   t >> 0

↤ Myo1a
||| Actin core
/ Apical membrane
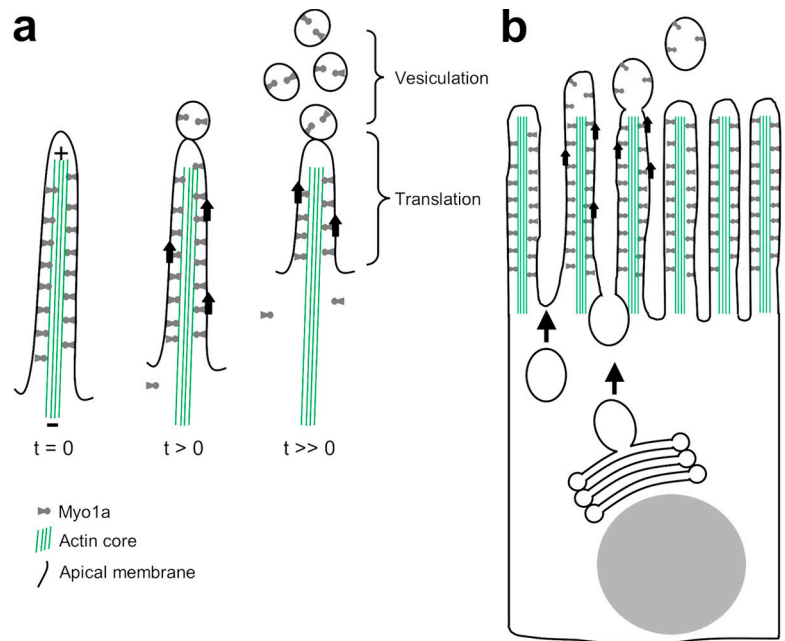
(Heintzelman et al., 1994) may also use core actin bundles as tracks for directed transport. Consistent with this idea, recent studies in the context of kidney proximal tubule reveal that hypertension induces the redistribution of Myo6 immunoreactivity along the microvillar axis (Yang et al., 2005). Our data also show that microvillar Myo1a is mechanochemically active and generates force in its native environment. This suggests that Myo1a may function as more than a passive "linker" serving to stabilize membrane/cytoskeleton interactions (Tyska et al., 2005). Finally, while general models for myosin-I function have always included some form of mechanical activity involving membrane rearrangement or movement (Coluccio, 1997; De La Cruz and Ostap, 2004), direct evidence for these functions has been lacking. The data presented here demonstrate directly, in a native system, that Myo1a is capable of producing mechanical forces sufficient to power the movement of cellular membranes over the actin cytoskeleton.

Physiological significance of BB membrane shedding

A number of previous biochemical studies have documented the existence of small vesicles in the lumen of the small intestine (Black et al., 1980; Jacobs, 1983; DeSchryver-Kecskemeti et al., 1989; Eliakim et al., 1989; Halbhuber et al., 1994; van Niel et al., 2001). Although these vesicles are enriched in nutrient-processing enzymes (e.g., SI and AP) in a manner similar to BB membrane, their mechanism of release remains unclear. Vesiculation from the tips of microvilli has also been captured in ultrastructural studies of intact enterocytes (Doughterty, 1976), suggesting that lumenal vesicles may originate from microvillar membrane. We propose that the Myo1a-dependent mechanical activity described in this paper provides a mechanism for the formation and release of vesicles from enterocyte BBs in vivo (Fig. 8 B). This model becomes even more appealing if we consider that membrane shedding from microvilli in vivo is

accelerated when enterocytes are treated with antibodies against SI (Lorenzsonn and Olsen, 1982), a transmembrane disaccharidase that interacts directly with Myo1a in a raft-like complex in the microvillar membrane (Tyska and Mooseker, 2004). The shedding of vesicles from the plasma membrane is a well-documented activity performed by a variety of epithelial cell types under normal and pathological conditions (Beaudoin and Grondin, 1991). In the gastrointestinal tract, the release of membrane vesicles laden with nutrient-processing enzymes could serve to increase the effective apical membrane surface area; such vesicles would allow processing to begin before nutrients reached the actual surface of the enterocyte (Jacobs, 1983). Others have proposed that BB membrane shedding may allow the enterocyte to continually modify its apical membrane composition (Halbhuber et al., 1994). This form of plasticity may be a critical aspect of the enterocyte response to the shifting demands in nutrient processing and absorption that are commonplace in the small intestine.

Does the membrane shedding process described here represent a general function for microvilli found on other polarized cell types? Although the expression of Myo1a is restricted to the gastrointestinal tract and inner ear (Skowron et al., 1998; Skowron and Mooseker, 1999; Dumont et al., 2002; Donaudy et al., 2003), other closely related class I myosins (Myo1b, Myo1c, and Myo1d) are more widely expressed in polarized cells from a variety of tissues (including kidney, liver, and pancreas) and in some cases are known to localize to microvilli (Coluccio, 1997). Interestingly, previous studies have established that all of these tissues release vesicles into their lumens (Beaudoin and Grondin, 1991). Thus, further studies are required to determine whether the activity described in this paper represents a general function for class I myosins expressed in other cell types, or a phenomenon specific to the gastrointestinal tract.

In recent studies with the Myo1a KO mouse, we observed herniations of the apical domain, where large regions of BB

membrane were detached from underlying microvillar actin bundles (Tyska et al., 2005). We originally proposed that these herniations arise due to a lack of membrane/cytoskeleton adhesion normally provided by Myo1a. However, our new findings suggest an alternative explanation: herniations may represent excess apical membrane in the BB. In KO enterocytes, the apical sorting machinery continues to deliver apical domain components to the BB. However, in the absence of Myo1a and its associated plus end–directed mechanical activity, membrane release from microvillar tips may be slowed, resulting in the accumulation of membrane in the BB, and ultimately the formation of membrane herniations.

The microvillar tip complex in BB membrane shedding

Early ultrastructural studies of the enterocyte BB revealed the presence of a prominent electron-dense plaque at the distal tips of microvilli (Mooseker and Tilney, 1975). To date, the role of the tip complex remains unclear, but by analogy to similar structures in stereocilia and filopodia, we suspect that at least one function may be in controlling the dimensions and dynamics of the core actin bundle (Lin et al., 2005). Does the tip complex also play a role in the process of membrane vesiculation from microvillar tips as described in this paper? It remains possible that an additional role for this complex may be in the formation of vesicles, perhaps through promoting and/or stabilizing the high curvature of membrane that envelops the microvillus tip. This would be analogous to the activity of viral proteins such as VSV-M, which are known to be involved in curving membrane through direct interactions with lipids (Solon et al., 2005). Alternatively, this complex may contain proteins that actively promote fission and vesicle release. In either case, the tip complex must be dynamically reassembled after vesicle release or somehow left behind during the process. The former idea finds support in recent proteomic studies (van Niel et al., 2001), which show that one of the few proteins known to localize to microvillar tips, Eps8 (Croce et al., 2004), is found in vesicles released from the apical surface of cultured intestinal epithelial cells.

The BB contains two actomyosin contractile arrays

Early experiments with isolated BBs established that ATP induced a contraction of the junctional band of actin filaments surrounding the terminal web region (Rodewald et al., 1976). A number of groups actively investigated this contractility and the involvement of Myo2, which at the time was the only known force generator in the BB (Rodewald et al., 1976; Burgess, 1982; Keller and Mooseker, 1982; Keller et al., 1985). The findings presented here demonstrate that terminal web contraction and microvillar membrane translation/shedding are independent and separable activities (Fig. 7, C and D). Thus, we propose that the BB contains two distinct actomyosin contractile arrays: (1) a Myo2-based array that powers the contraction of the junctional band surrounding the terminal web region, and (2) a Myo1a-based array in microvilli that exerts plus end–directed forces on the apical membrane (Fig. 8 A).

Myo1a was first visualized in microvilli in the form of lateral bridges (Mooseker and Tilney, 1975) at about the same time the early studies on BB contractility began (around 1976; Rodewald et al., 1976). However, the motor properties of Myo1a were not discovered until the late 1980s (Mooseker and Coleman, 1989). We believe that this lag in the experimental timeline may explain why microvillar membrane translation and shedding were not described before this work. Interestingly, evidence of ATP-induced membrane vesiculation consistent with that reported here can indeed be seen in ultramicrographs from studies on isolated BBs and microvilli performed before Myo1a was recognized as a bona fide motor protein (Rodewald et al., 1976; Howe and Mooseker, 1983; Verner and Bretscher, 1983).

Concluding remarks

The classic view of microvillar function suggests these structures serve to enhance the efficiency of nutrient uptake by amplifying the apical membrane surface area available for nutrient processing and absorption. The work presented here suggests that microvilli also function as actomyosin contractile arrays, allowing for the plus end–directed movement and shedding of BB membrane from microvillar tips. Because this process may have considerable implications with regard to gastrointestinal physiology, future studies will focus on investigating how Myo1a contributes to BB membrane shedding in vivo.

Materials and methods

BB isolation

BBs were collected with a modification of the method of Howe and Mooseker (1983). All procedures involving animals were performed under the auspices of Vanderbilt University Medical Center (VUMC) Institutional Animal Care and Use Committee. All chemicals were obtained from Sigma-Aldrich unless otherwise noted. Intestines were dissected from adult animals (Sprague-Dawley rats or wild-type/Myo1a KO mice), flushed with ice-cold saline (150 mM NaCl, 2 mM imidazole-Cl, and 0.02% Na-Azide), and stirred in dissociation solution (DS; 200 mM sucrose, 0.02% Na-Azide, 12 mM EDTA-K, 18.9 mM KH_2PO_4, and 78 mM Na_2HPO_4, pH 7.2) for 20 min. Released cells were washed with multiple cycles of sedimentation (200 g for 10 min; X-15R centrifuge, Beckman Coulter) and resuspension in fresh DS. Cleaned cell pellets were resuspended in homogenization buffer (HB; 10 mM imidazole, 4 mM EDTA-K, 1 mM EGTA-K, 0.02% Na-Azide, 1 mM DTT, and 1 mM Pefabloc-SC, pH 7.2) and homogenized in a Waring blender with 4×15-s pulses. BBs were collected from the homogenate by centrifugation at 1,000 g for 10 min; BB pellets were then washed in solution A (75 mM KCl, 10 mM imidazole, 1 mM EGTA, 5 mM $MgCl_2$, and 0.02% Na-Azide, pH 7.2) and sucrose was added to 50% final concentration. Samples were overlayed with 40% sucrose and centrifuged at 130,000 g for 1 h at 4°C in an ultracentrifuge (L8-70M; Beckman Coulter). BBs were collected from the 40/50% interface, resuspended in solution B (150 mM KCl, 20 mM imidazole, 2 mM EGTA, 5 mM $MgCl_2$, 0.02% Na-Azide, 1 mM DTT, and 1 mM Pefabloc-SC, pH 7.2), and stored on ice. Protein concentrations were determined using the Coomassie Blue Assay (Pierce Chemical Co.).

Confocal microscopy

Isolated BBs were incubated in solution B in the presence or absence of 2 mM ATP for 5 min at room temperature, then fixed for 15 min at room temperature with 4% paraformaldehyde in PBS (137 mM NaCl, 7 mM Na_2HPO_4, and 3 mM NaH_2PO_4, pH 7.2). BBs were then washed with fresh PBS, stained with Alexa488-phalloidin (1:200) and either TRITC-ConA (1:200; Molecular Probes) or AM1-43 (1:100; Biotium Inc.) overnight on ice. BBs were washed three times in PBS and mounted on slides. Confocal micrographs were acquired on a laser scanning confocal microscope (FV-1000; Olympus) (100×/1.3 N.A. Plan Apo objective). All images were contrast enhanced, pseudo-colored, and cropped using

ImageJ software (v. 1.36b; National Institutes of Health, Bethesda, MD); figures were assembled using PowerPoint X (Microsoft). Pearson correlation values were calculated from BB confocal images as follows. In brief, red and green color channels were separated and converted to 8-bit grayscale images. Each image was normalized with the Enhance Contrast function, such that 0.5% of all pixels achieved saturation. Correlation coefficients were then extracted using the Colocalization Finder plug-in (C. Laummonerie and J. Mutterer, Institute of Plant Molecular Biology, Strasbourg, France).

Time-lapse light microscopy
For time-lapse microscopy, BBs in solution B were added to flow cells constructed of #1 cover glass (Corning) separated by two parallel strips of double-sided Scotch tape and allowed to adsorb the glass surface for 2 min at room temperature. Loosely bound and unbound BBs were washed out of the flow cell with several volumes of fresh solution B. Flow cells were imaged using an inverted microscope (TE2000; Nikon) equipped with either DIC optics (100×/1.3 N.A. Plan Fluor objective, CoolSnap HQ CCD camera [Roper Scientific], ImagePro Express software [Media Cybernetics]), or a spinning disk confocal head (QLC100; Visitech) (100×/1.4 N.A. Plan Apo objective, Cascade 512B CCD camera [Roper Scientific], IPLab software [BD Biosciences]). Images used to calculate velocity histogram data were acquired on a Leica TCS SP5 laser-scanning confocal (63×/1.4 N.A. Plan Apo objective). To activate BBs, solution B supplemented with 2 mM ATP was pipetted into the flow cell during image acquisition. Montages of time-lapse data were created using ImageJ, and kymographs were generated using the ImageJ Multiple Kymograph plug-in (J. Rietdorf and A. Seitz, European Molecular Biology Laboratory, Heidelberg, Germany).

Biochemical isolation of shed membrane
BBs (200 μg total protein) were suspended in solution B and incubated with or without 2 mM ATP for 10 min at room temperature. Samples were centrifuged at 5,000 g for 10 min at 4°C to separate shed membrane (supernatant) from intact BBs and BB fragments (pellet). To isolate the shed membrane vesicles, the 5,000-g supernatant was spun at 100,000 g for 2 h at 4°C in an ultracentrifuge (TL-100; Beckman Coulter) using a TLA 120.2 rotor. 5,000- and 100,000-g pellets were resuspended in solution B to volumes equivalent to the original reaction. The resulting fractions were prepared for immunoblot analysis and electron microscopy as described below.

Electron microscopy
All EM reagents were purchased from Electron Microscopy Sciences. For the ultrastructural examination of ATP-treated BBs, BBs were incubated in solution B in the presence or absence of 2 mM ATP for 5 min at room temperature. BBs were fixed in 0.1 M Na-phosphate buffer (pH 7.0) containing 2% glutaraldehyde and 2 mg/ml Tannic acid on ice for 1 h. BB were washed with 0.1 M Na-phosphate buffer (pH 7.0) and post-fixed with 1% OsO_4 in 0.1 M Na-phosphate buffer (pH 6.0) for 30 min on ice. BBs were then washed in cold water and stained overnight in 1% uranyl acetate. Samples were then dehydrated with a graded ethanol series followed by 100% propylene dioxide. BBs were infiltrated with a 1:1 epon/propylene dioxide mix for 6 h, and then placed in fresh EPON for 2 h and baked at 60°C overnight. Ultrathin sections were cut on an ultra-microtome (Leica). For negative stain, BB fractions were deposited on Formvar coated grids and stained with 1% uranyl acetate. All grids were imaged on a transmission electron microscope (CM12; Phillips) equipped with 8-bit grayscale digital image capture capabilities (1024 × 1184 pixels).

SDS-PAGE and immunoblot analysis
Protein fractions were separated using NuPAGE Bis-Tris 4–12% gradient gels (Invitrogen) run in Morpholineethanesulfonic acid buffer. Proteins were transferred to nitrocellulose membranes at 30V overnight at 4°C. Stock solutions of primary antibodies were used as follows: anti-Myo1a (CX-1 ascites fluid; a gift from Mark Mooseker, Yale University, New Haven, CT; Carboni et al., 1988), anti–rat SI (a gift from Andreas Quaroni, Cornell University, Ithaca, NY), and anti-CaM (Upstate Biotechnologies) were all diluted 1:1,000; anti-AP (Sigma-Aldrich) was diluted 1:2,500. Secondary antibodies (Promega) were diluted 1:5,000. Immunogens were visualized using ECL reagents according to manufacturer's protocol (GE Healthcare).

Membrane shedding assay
BBs were stained with AM1-43 (1:100; Biotium Inc.) and unlabeled phalloidin (1:100; Invitrogen) overnight on ice, and then washed with fresh

solution B to remove excess dye. Shedding assay reactions were performed in triplicate; BBs were resuspended in solution B at 0.02 mg/ml and then stimulated with the addition of ATP (or other ligands as indicated) to 2 mM. Reactions were incubated for 2 min at room temperature and then subject to centrifugation at 5000 g for 5 min at 4°C. The resulting 5,000-g supernatant was transferred to a flat-bottomed, 96-well plate (Corning) and fluorescence was measured using a microplate reader (Synergy HT; Bio-Tek) using 485/15-nm excitation and 590/20-nm emission detection. Detector gain was set so that the brightest well was near the upper limit of the detector range. Control BBs (not exposed to ATP) were processed in parallel and provided an estimate of the reaction background. For each condition, the triplicate fluorescence values were averaged and background subtracted to derive the ATP-dependent response. Nucleotide analogues ATP-γS and AMP-PNP were purchased from Roche Applied Science or Sigma-Aldrich.

Statistical Analysis
A t test was used to analyze data in Fig. 1. A Mann-Whitney test for unpaired data was used to analyze data in Fig. 7; $P < 0.05$ was considered significant.

Online supplemental material
Video 1 shows time-lapse DIC microscopy of an isolated BB shedding membrane in response to ATP. Video 2 shows time-lapse spinning disk confocal microscopy of two isolated BBs shedding membrane in response to ATP. Online supplemental material is available at http://www.jcb.org/cgi/content/full/jcb.200701144/DC1.

References

Beaudoin, A.R., and G. Grondin. 1991. Shedding of vesicular material from the cell surface of eukaryotic cells: different cellular phenomena. *Biochim. Biophys. Acta.* 1071:203–219.

Belyantseva, I.A., E.T. Boger, and T.B. Friedman. 2003. Myosin XVa localizes to the tips of inner ear sensory cell stereocilia and is essential for staircase formation of the hair bundle. *Proc. Natl. Acad. Sci. USA.* 100:13958–13963.

Berg, J.S., and R.E. Cheney. 2002. Myosin-X is an unconventional myosin that undergoes intrafilopodial motility. *Nat. Cell Biol.* 4:246–250.

Black, B.L., Y. Yoneyama, and F. Moog. 1980. Microvillous membrane vesicle accumulation in media during culture of intestine of chick embryo. *Biochim. Biophys. Acta.* 601:343–348.

Bretscher, A. 1991. Microfilament structure and function in the cortical cytoskeleton. *Annu. Rev. Cell Biol.* 7:337–374.

Burgess, D.R. 1982. Reactivation of intestinal epithelial cell brush border motility: ATP-dependent contraction via a terminal web contractile ring. *J. Cell Biol.* 95:853–863.

Carboni, J.M., K.A. Conzelman, R.A. Adams, D.A. Kaiser, T.D. Pollard, and M.S. Mooseker. 1988. Structural and immunological characterization of the myosin-like 110-kD subunit of the intestinal microvillar 110K-calmodulin complex: evidence for discrete myosin head and calmodulin-binding domains. *J. Cell Biol.* 107:1749–1757.

Coluccio, L.M. 1997. Myosin I. *Am. J. Physiol.* 273:C347–C359.

Cremo, C.R., and M.A. Geeves. 1998. Interaction of actin and ADP with the head domain of smooth muscle myosin: implications for strain-dependent ADP release in smooth muscle. *Biochemistry.* 37:1969–1978.

Croce, A., G. Cassata, A. Disanza, M.C. Gagliani, C. Tacchetti, M.G. Malabarba, M.F. Carlier, G. Scita, R. Baumeister, and P.P. Di Fiore. 2004. A novel actin barbed-end-capping activity in EPS-8 regulates apical morphogenesis in intestinal cells of *Caenorhabditis elegans. Nat. Cell Biol.* 6:1173–1179.

De La Cruz, E.M., and E.M. Ostap. 2004. Relating biochemistry and function in the myosin superfamily. *Curr. Opin. Cell Biol.* 16:61–67.

DeSchryver-Kecskemeti, K., R. Eliakim, S. Carroll, W.F. Stenson, M.A. Moxley, and D.H. Alpers. 1989. Intestinal surfactant-like material. A novel secretory product of the rat enterocyte. *J. Clin. Invest.* 84:1355–1361.

Donaudy, F., A. Ferrara, L. Esposito, R. Hertzano, O. Ben-David, R.E. Bell, S. Melchionda, L. Zelante, K.B. Avraham, and P. Gasparini. 2003. Multiple mutations of MYO1A, a cochlear-expressed gene, in sensorineural hearing loss. *Am. J. Hum. Genet.* 72:1571–1577.

Doughterty, W.J. 1976. Microblebs of intestinal epithelial cell microvilli of *Citellus tridecemlineatus*. *Anat. Rec.* 185:77–83.

Dumont, R.A., Y.D. Zhao, J.R. Holt, M. Bahler, and P.G. Gillespie. 2002. Myosin-I isozymes in neonatal rodent auditory and vestibular epithelia. *J. Assoc. Res. Otolaryngol.* 3:375–389.

Eliakim, R., K. DeSchryver-Kecskemeti, L. Nogee, W.F. Stenson, and D.H. Alpers. 1989. Isolation and characterization of a small intestinal surfactant-like particle containing alkaline phosphatase and other digestive enzymes. *J. Biol. Chem.* 264:20614–20619.

Halbhuber, K.J., M. Schulze, H. Rhode, R. Bublitz, H. Feuerstein, M. Walter, W. Linss, H.W. Meyer, and A. Horn. 1994. Is the brush border membrane of the intestinal mucosa a generator of "chymosomes"? *Cell Mol. Biol. (Noisy-le-grand).* 40:1077–1096.

Hayden, S.M., J.S. Wolenski, and M.S. Mooseker. 1990. Binding of brush border myosin I to phospholipid vesicles. *J. Cell Biol.* 111:443–451.

Heintzelman, M., T. Hasson, and M. Mooseker. 1994. Multiple unconventional myosin domains of the intestinal brush border cytoskeleton. *J. Cell Sci.* 107:3535–3543.

Howard, J. 2001. Mechanics of Motor Proteins and the Cytoskeleton. Sinauer Associates, Inc., New York. 384 pp.

Howe, C.L., and M.S. Mooseker. 1983. Characterization of the 110-kdalton actin-calmodulin-, and membrane-binding protein from microvilli of intestinal epithelial cells. *J. Cell Biol.* 97:974–985.

Jacobs, L.R. 1983. Biochemical and ultrastructural characterization of the molecular topography of the rat intestinal microvillous membrane. Asymmetric distribution of hydrophilic groups and anionic binding sites. *Gastroenterology.* 85:46–54.

Jontes, J.D., R.A. Milligan, T.D. Pollard, and E.M. Ostap. 1997. Kinetic characterization of brush border myosin-I ATPase. *Proc. Natl. Acad. Sci. USA.* 94:14332–14337.

Kelemen, G.S. 1979. Kinetic study of the inhibition of myosin ATPase activity by ADP. *Acta Biochim. Biophys. Acad. Sci. Hung.* 14:241–248.

Keller, T.C., and M.S. Mooseker. 1982. Ca++-calmodulin-dependent phosphorylation of myosin, and its role in brush border contraction in vitro. *J. Cell Biol.* 95:943–959.

Keller, T.C., K.A. Conzelman, R. Chasan, and M.S. Mooseker. 1985. Role of myosin in terminal web contraction in isolated intestinal epithelial brush borders. *J. Cell Biol.* 100:1647–1655.

Kovacs, M., J. Toth, C. Hetenyi, A. Malnasi-Csizmadia, and J.R. Sellers. 2004. Mechanism of blebbistatin inhibition of myosin II. *J. Biol. Chem.* 279:35557–35563.

Lin, H.W., M.E. Schneider, and B. Kachar. 2005. When size matters: the dynamic regulation of stereocilia lengths. *Curr. Opin. Cell Biol.* 17:55–61.

Lorenzsonn, V., and W.A. Olsen. 1982. In vivo responses of rat intestinal epithelium to intraluminal dietary lectins. *Gastroenterology.* 82:838–848.

Mooseker, M.S., and L.G. Tilney. 1975. Organization of an actin filament-membrane complex. Filament polarity and membrane attachment in the microvilli of intestinal epithelial cells. *J. Cell Biol.* 67:725–743.

Mooseker, M.S., and C.L. Howe. 1982. The brush border of intestinal epithelium: a model system for analysis of cell-surface architecture and motility. *Methods Cell Biol.* 25:143–174.

Mooseker, M.S., and T.R. Coleman. 1989. The 110-kD protein-calmodulin complex of the intestinal microvillus (brush border myosin I) is a mechanoenzyme. *J. Cell Biol.* 108:2395–2400.

Revenu, C., R. Athman, S. Robine, and D. Louvard. 2004. The co-workers of actin filaments: from cell structures to signals. *Nat. Rev. Mol. Cell Biol.* 5:635–646.

Rodewald, R., S.B. Newman, and M.J. Karnovsky. 1976. Contraction of isolated brush borders from the intestinal epithelium. *J. Cell Biol.* 70:541–554.

Rzadzinska, A.K., M.E. Schneider, C. Davies, G.P. Riordan, and B. Kachar. 2004. An actin molecular treadmill and myosins maintain stereocilia functional architecture and self-renewal. *J. Cell Biol.* 164:887–897.

Skowron, J.F., and M.S. Mooseker. 1999. Cloning and characterization of mouse brush border myosin-I in adult and embryonic intestine. *J. Exp. Zool.* 283:242–257.

Skowron, J.F., W.M. Bement, and M.S. Mooseker. 1998. Human brush border myosin-I and myosin-Ic expression in human intestine and Caco-2BBe cells. *Cell Motil. Cytoskeleton.* 41:308–324.

Solon, J., O. Gareil, P. Bassereau, and Y. Gaudin. 2005. Membrane deformations induced by the matrix protein of vesicular stomatitis virus in a minimal system. *J. Gen. Virol.* 86:3357–3363.

Straight, A.F., A. Cheung, J. Limouze, I. Chen, N.J. Westwood, J.R. Sellers, and T.J. Mitchison. 2003. Dissecting temporal and spatial control of cytokinesis with a myosin II Inhibitor. *Science.* 299:1743–1747.

Tyska, M.J., and M.S. Mooseker. 2004. A role for myosin-1A in the localization of a brush border disaccharidase. *J. Cell Biol.* 165:395–405.

Tyska, M.J., A.T. Mackey, J.D. Huang, N.G. Copeland, N.A. Jenkins, and M.S. Mooseker. 2005. Myosin-1a is critical for normal brush border structure and composition. *Mol. Biol. Cell.* 16:2443–2457.

van Niel, G., G. Raposo, C. Candalh, M. Boussac, R. Hershberg, N. Cerf-Bensussan, and M. Heyman. 2001. Intestinal epithelial cells secrete exosome-like vesicles. *Gastroenterology.* 121:337–349.

Verner, K., and A. Bretscher. 1983. Induced morphological changes in isolated microvilli: regulation of membrane topology in vitro by submembranous microfilaments. *Eur. J. Cell Biol.* 29:187–192.

Warshaw, D.M., J.M. Desrosiers, S.S. Work, and K.M. Trybus. 1991. Effects of MgATP, MgADP, and Pi on actin movement by smooth muscle myosin. *J. Biol. Chem.* 266:24339–24343.

Wolenski, J.S., R.E. Cheney, P. Forscher, and M.S. Mooseker. 1993a. In vitro motilities of the unconventional myosins, brush border myosin-I, and chick brain myosin-V exhibit assay-dependent differences in velocity. *J. Exp. Zool.* 267:33–39.

Wolenski, J.S., S.M. Hayden, P. Forscher, and M.S. Mooseker. 1993b. Calcium-calmodulin and regulation of brush border myosin-I MgATPase and mechanochemistry. *J. Cell Biol.* 122:613–621.

Yang, L.E., A.B. Maunsbach, P.K. Leong, and A.A. McDonough. 2005. Redistribution of myosin VI from top to base of proximal tubule microvilli during acute hypertension. *J. Am. Soc. Nephrol.* 16:2890–2896.

Zot, H.G. 1995. Phospholipid membrane-associated brush border myosin-I activity. *Cell Motil. Cytoskeleton.* 30:26–37.